Journal of The Electrochemical Society, **150** (2) F7-F10 (2003)
0013-4651/2003/150(2)/F7/4/$7.00 © The Electrochemical Society, Inc.

Electrical Transport Phenomena in Aromatic Hydrocarbon Polymer

Po-Tsun Liu,[a,*,z] T. C. Chang,[a,b,] Shuo-Ting Yan,[c] Chun-Huai Li,[c] and S. M. Sze[a,c]**

[a]*National Nano Device Laboratory, HsinChu 300, Taiwan*
[b]*Department of Physics, National Sun Yat-Sen University, Taiwan*
[c]*Institute of Electronics, National Chiao Tung University, Taiwan*

Electrical transport mechanisms in a low-permittivity aromatic hydrocarbon SiLK have been characterized using metal/SiLK/Si capacitors under both thermal and electric field stressing. Two distinct transport mechanisms dominate the leakage behavior of the polymer SiLK with Al and Cu electrodes, respectively. Al-electrode capacitors show Schottky-emission (SE)-type leakage behavior while Poole-Frenkel (PF) conduction resulted from trap generation in the SiLK polymer is responsible for the leakage of Cu-electrode capacitors. The trap barrier height has been extracted from the temperature dependence of leakage current. Copper penetration into the SiLK polymer leads to the generation of trap centers and seriously deteriorates dielectric characteristics. The transition of leakage conduction from SE to PF will exponentially lead to the insulating failure of the SiLK polymer.
 [DOI: 10.1149/1.1535204]

Manuscript submitted March 11, 2002; revised manuscript received May 31, 2002. Available electronically January 6, 2003.

As the scale of microelectronic devices continues to shrink, back-end-of-line (BEOL) interconnect delay increasingly dominates the performance of integrated circuits (IC). The implementation of integrating copper wiring with low-permittivity (low-*k*) dielectrics can effectively reduce resistance-capacitance (RC) delay as well as increasing electromigration resistance.[1] A variety of low-*k* candidates including silicate-based and aromatic-based materials have emerged to meet the dielectric requirements.[2-7] An aromatic hydrocarbon thermosetting polymer, SiLK, which has a low dielectric constant, low moisture uptake, and high fracture toughness[7] is receiving much attention for 0.13 μm and below BEOL applications.[8,9]

With the advent of copper technology, dual damascene processes have been developed to facilitate patterning of copper interconnects. The damascene processes need to place large demands on dielectric material integrity, such as withstanding more aggressive bias-temperature stress, and minimizing metal diffusion; otherwise, once metal ions penetrate through inadequate barrier layers into low-*k* dielectrics, intrinsic dielectric property will dominate the electrical performance of the interconnect system. For example, it will influence leakage current and premature breakdown of the dielectrics significantly.[10] Thus, the electrically intrinsic characteristic of low-*k* dielectrics is one of the important factors for reliability considerations and requires to be assessed carefully.

In general, the electrically intrinsic parameters such as breakdown voltage, intra- and intermetal leakage current are predominately determined by the conduction mechanisms in the dielectrics. Also, the energy barrier at the metal/dielectric interfaces might control the electron injection from metal into the dielectrics. The knowledge of the nature of the carrier transport could give interesting information on leakage behavior and the origin of the breakdown processes. Nevertheless, the conduction mechanism on the low-*k* aromatic polymer, specifically on the SiLK material, is not completely understood yet.

In this work, we investigated the leakage characteristics of Al/SiLK/Si and Cu/SiLK/Si capacitors under temperature and electrical stressing. Specially, the leakage transport mechanisms have been analyzed in detail by extracting the information from their electrical characteristics.

Experimental

The p-type single crystal silicon wafers with (100) orientation were spin coated with a single layer of SiLK film and baked on a hot plate at 300°C for 90 s. It was followed by furnace curing at 400°C for 1 h under nitrogen atmosphere. Metal-insulator-semiconductor capacitors (MIS) were manufactured by sputtering aluminum and copper layer on SiLK films, respectively, as the top electrode. Then, an aluminum layer was sequentially deposited on the back side of the substrates for electrically good contact.

In realistic operation of integrated circuits, devices work under both higher temperatures than room temperature and relatively high electric fields. To simulate the rigorous conditions, bias temperature stressing (BTS) and electrical measurements at high temperatures were conducted on these metal/SiLK/Si capacitors. The test samples were vacuum held on an MSI Electronics light/hot chuck and were under nitrogen purge throughout the stressing. BTS experiments

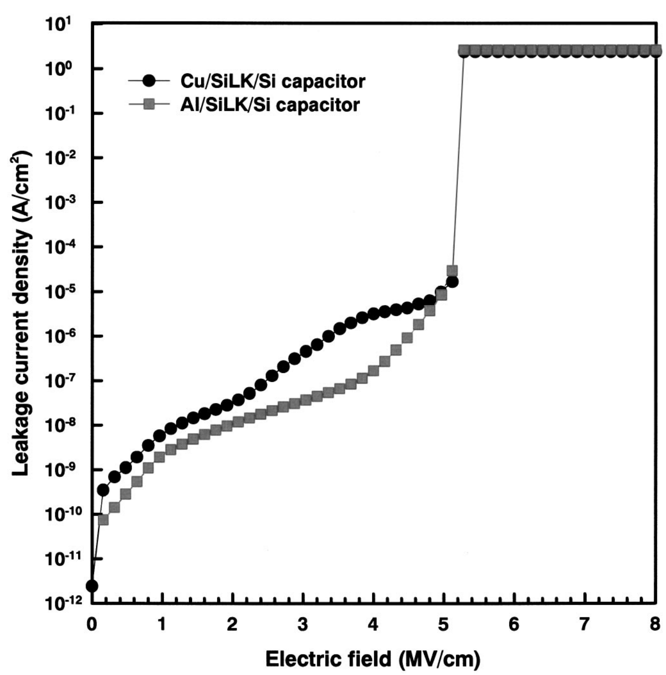

Figure 1. Leakage current density of SiLK films with Al and Cu electrodes after a BTS test. The BTS experiments were performed at 170°C for 1000 s under a electric field of 1 MV/cm.

* Electrochemical Society Student Member.
** Electrochemical Society Active Member.
[z] E-mail: ptliu@ndl.gov.tw

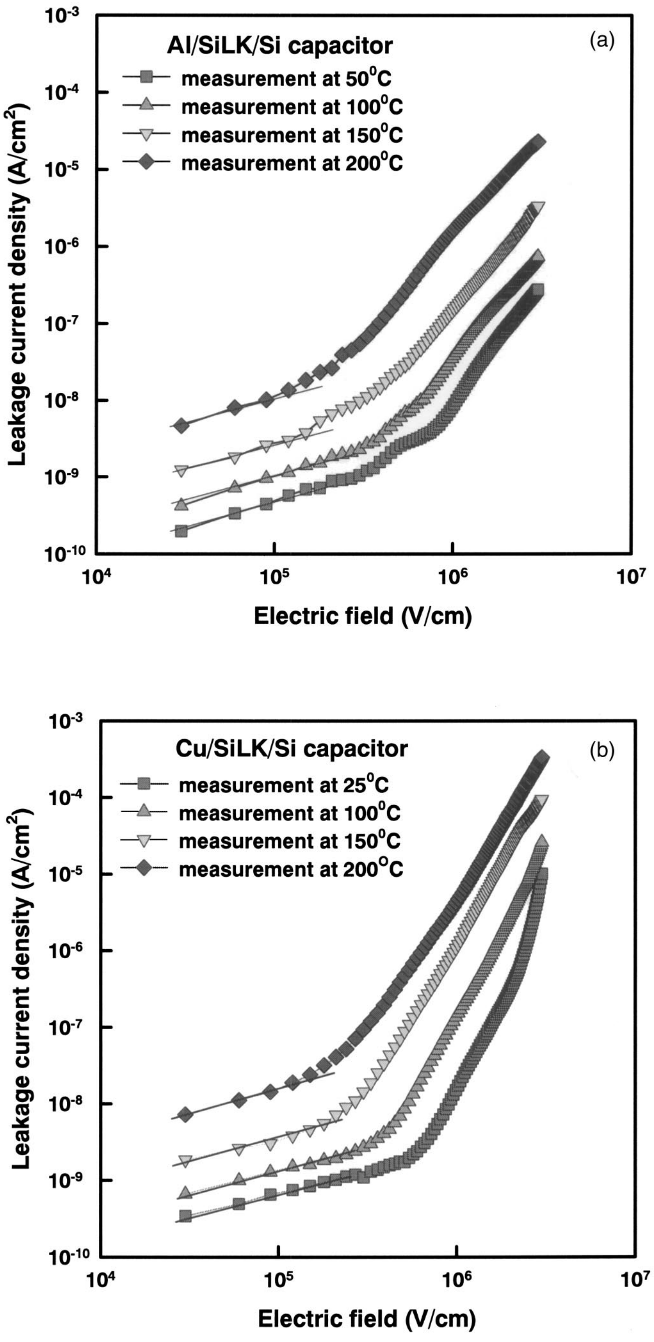

Figure 2. Log J *vs.* log E characteristics of SiLK films with (a) Al and (b) Cu metal electrode, measured at 50, 100, 150, and 200°C. The linear lines in Fig. 2a and b show the nearly ohmic conduction at the low field ($<1.5 \times 10^{15}$ V/cm).

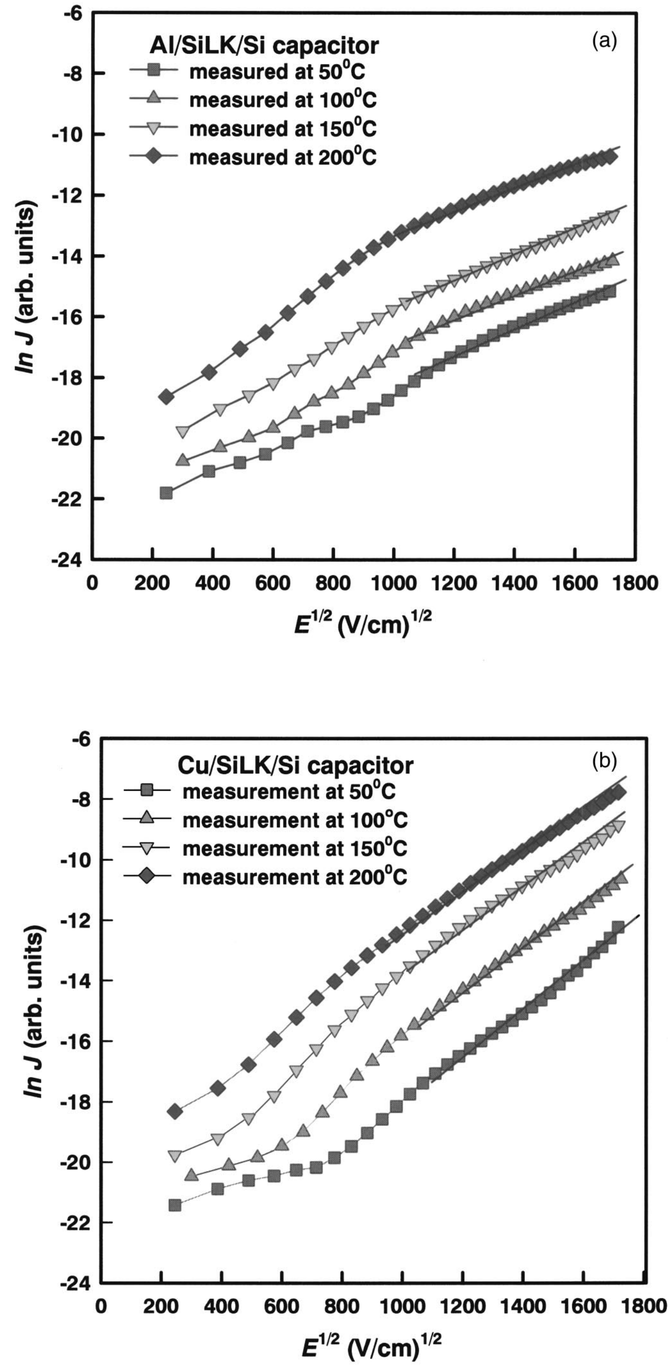

Figure 3. J-E curves on a ln J *vs.* $E^{1/2}$ plot of the SiLK films with (a) Al and (b) Cu electrode, measured at 50, 100, 150, and 200°C. The leakage current densities are linearly related to square root of the applied electric field, higher than 1 MV/cm. Fitting with a SE current is shown in Fig. 3a and a PF-type current in Fig. 3b.

were performed at 170°C for 1000 s under a electric field of 1 MV/cm. Electrical measurements, leakage current density *vs.* electric field (J-E), were performed at a variety of temperatures ranging from 50 to 200°C, using a semiconductor model HP4156 parameter analyzer. The dielectric constants of SiLK films were determined by high frequency capacitance-voltage (C-V) curves measured at 1 MHZ with an ac bias.

Results and Discussion

In the initial studies, the BTS testing was performed on the SiLK film to understand its impact on electrical characteristics. Figure 1 shows the leakage current of SiLK films with Al and Cu electrodes, respectively, following the BTS test. A significant difference between Al and Cu electrode capacitors appears in the leakage current characteristics. It is specially that the leakage current of Cu electrode capacitors is higher than that of the Al electrode capacitors. In addition, the endurance of Cu electrode capacitors to dielectric breakdown is inferior to that of Al electrode capacitors. For Al/SiLK/Si capacitors, the breakdown electric field (E_{BD}), which is defined as the electric field at which the leakage current density exceeds 1 $\mu A/cm^2$, is 4.5 MV/cm while Cu electrode capacitors have a lower E_{BD} at around 3.2 MV/cm. These results for Cu elec-

Table I. Various values of the constant β at 50°C, 100°C, 150°C, and 200°C.

Temperature (°C)		50	100	150	200
Al-gate SiLK	Experimental β	3.82×10^{-23}	3.75×10^{-23}	3.80×10^{-23}	3.72×10^{-23}
Cu-gate SiLK	Experimental β	7.60×10^{-23}	7.48×10^{-23}	7.45×10^{-23}	7.41×10^{-23}
Theoretical ε		2.6			
Theoretical β_s ($J\ cm^{1/2}/V^{1/2}$)		3.76×10^{-23}			
Theoretical β_{PF} ($J\ cm^{1/2}/V^{1/2}$)		7.53×10^{-23}			

trode capacitors are attributed to the injection of copper ions into the SiLK polymer, deteriorating its dielectric quality.[11] The origin of leakage current and electrical degradation originated from Cu penetration can be deduced further by analyzing leakage behavior of the SiLK polymer.

In order to elucidate the leakage mechanisms, electrical measurements at varied temperatures were conducted on Al/SiLK/Si and Cu/SiLK/Si capacitors. Figure 2 shows the log J − log E curves of Al and Cu electrode capacitors measured at temperatures ranging from 50 to 200°C. It is initially observed that in the low initial electric field region ($<5 \times 10^5$ V/cm), the leakage current density is linearly related to the applied field. The linear portion of the log J *vs.* log E curve is typical of ohmic conduction in low electric field and is dependent on charged carriers such as electrons and ions in the intrinsic aromatic hydrocarbon polymer. In addition, both leakage current densities of Al and Cu electrode capacitors are increased with increasing temperatures, revealing a temperature dependence on the leakage behavior. Comparing Al with Cu electrode capacitors under all test conditions, leakage current values in the low electric field region are close, whereas those in the high electric field region ($>10^6$ V/cm) reveal significant divergence. Especially, the leakage currents of Cu/SiLK/Si capacitors are higher than that of Al/SiLK/Si capacitors over the high electric fields extending from 1 to 3 MV/cm. A plot of the leakage current density *vs.* the square root of the applied electric field gives a good representation of the leakage conduction behavior in the high electric fields (>1 MV/cm), as shown in Fig. 3. Figures 3a and b show ln J and $E^{1/2}$ characteristic curves of the Al/SiLK/Si and Cu/SiLK/Si capacitors. We found that both leakage current densities are linearly related to square root of the applied electric field. These linear variations of current densities correspond either to Schottky emission (SE) or to Poole-Frenkel (PF) type conduction mechanism.[12]

The electrical characteristic in the SE can be quantified as follows

$$J = A^* T^2 \exp\left(\frac{\beta_s E^{1/2} - \phi_s}{k_B T}\right) \qquad [1]$$

where $\beta_s = (e^3/4\pi\varepsilon_0\varepsilon)^{1/2}$, e the electronic charge, ε_0 the dielectric constant of free space, ε the high frequency relative dielectric constant, A^* effective Richardson constant, T absolute temperature, ϕ_s the contact potential barrier, and k_B the Boltzmann constant.

The PF dominated current density is given as follows

$$J = J_0 \exp\left(\frac{\beta_{PF} E^{1/2} - \phi_{PF}}{k_B T}\right) \qquad [2]$$

where $J_0 = \sigma_0 E$ is the low field current density, σ_0 the low field conductivity, $\beta_{PF} = (e^3/\pi\varepsilon_0\varepsilon)^{1/2}$, ϕ_{PF} the height of trap potential well.

To distinguish SE from PF, the slopes ($\beta/k_B T$) of the curve ln J-$E^{1/2}$ were extracted for analysis. The various values of the constant β for Al and Cu electrode capacitors are summarized in Table I. The various values of β extracted from Al electrode capacitors are close to the theoretical β_s while those values of β extracted from Cu electrode capacitors are closer to the theoretical β_{PF} than β_s. These results indicate carriers are transported through the Al/SiLK/Si capacitors by the interface-dominated SE, whereas Cu electrode capacitors by trap-assisted PF mechanism instead. Schottky emission is due to the thermionic effect that is caused by the electron transport across the potential energy barrier via field-assisted lowering at the interface between metallic Al and low-k SiLK. Rearranging Eq. 1 into a relationship between ln(J/T^2) and $1/T$ can be used to calculate the Schottky barrier height ϕ_s

$$\ln\frac{J}{T^2} = \ln A^* - \frac{1}{T}\left(\frac{\phi_s}{k_B} - \frac{\beta_s\sqrt{E}}{k_B}\right) \qquad [3]$$

The ln(J/T^2) *vs.* $1/T$ plot shown in Fig. 4 clearly fits to a straight line as expected for a thermionic emission. Also, the slope of the plot indicates a Schottky barrier height of $e\phi_s = 0.60$ eV.

As is the case of Cu/SiLK/Si capacitors, the PF emission is caused by field-enhanced thermal excitation of trapped electrons in SiLK into the conduction band. The trap centers are largely generated in SiLK because of copper driving in the SiLK film[11] under the aggressive test conditions. The trap-assisted conduction behavior leads to an obvious increase in leakage current with increasing tem-

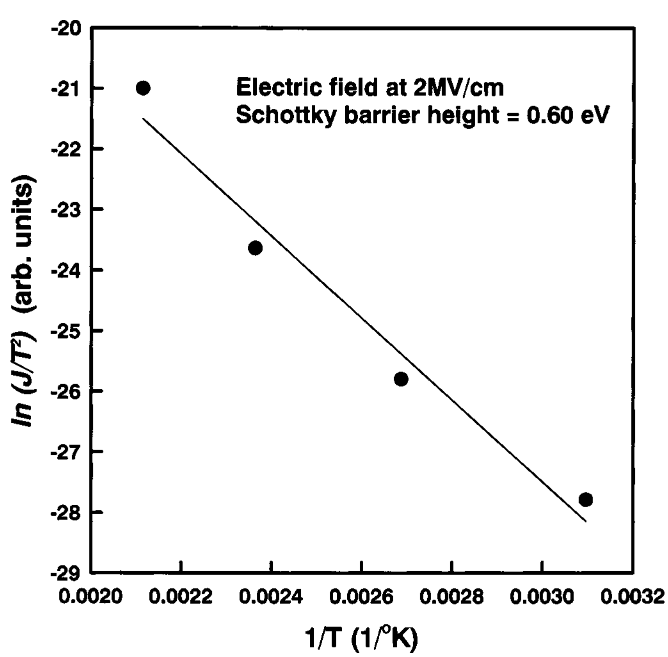

Figure 4. Temperature dependence of the SE-dominated leakage current. The Schottky barrier height, $e\phi_s$, is 0.60 eV extracted from the slope of the linear ln J/T^2 − $1/T$ plot.

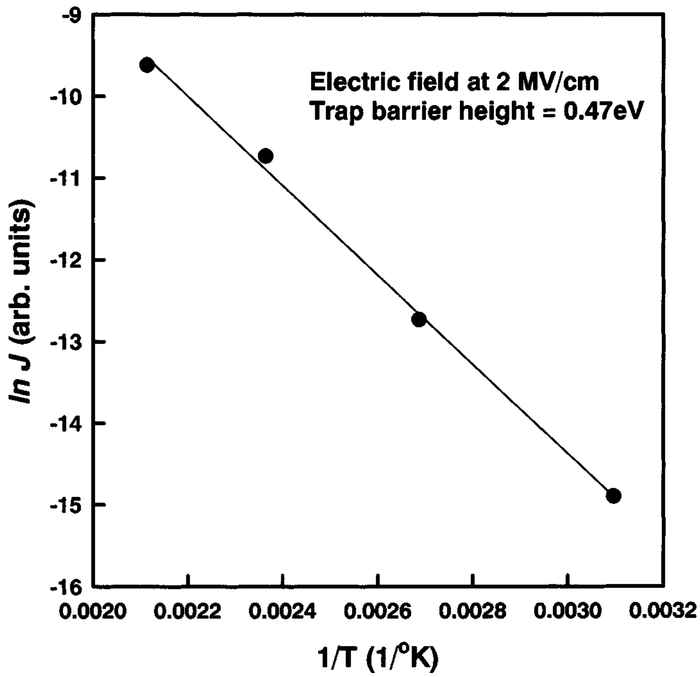

Figure 5. Temperature dependence of the PF-type leakage current. The trap height $e\phi_{PF}$ for PF conduction leakage is 0.47 eV.

peratures. Rearrangement of Eq. 2 also yields a linear relationship between ln J and $1/T$, capable of calculating the height of trap potential well ϕ_{PF}

$$\ln J = \ln(J_0) - \frac{1}{T}\left(\frac{\phi_{PF}}{k_B} - \frac{\beta_{PF}\sqrt{E}}{k_B}\right) \qquad [4]$$

As shown in Fig. 5, the value of $e\phi_{PF}$ extracted from the slope of the ln J-$1/T$ straight line is around 0.47 eV, which is lower than the Schottky barrier height (0.60 eV) in the case of Al contact. Since the activation energy of leakage conduction in Cu/SiLK/Si capacitors is lower than that of Al/SiLK/Si capacitors, the tendency to electrical degradation is relatively significant in the Cu electrode capacitors. Even the electrical insulation of the SiLK polymer will reduce exponentially by the power of two, due to $\beta_{PF} = 2\beta_s$, while switching metallic Al to Cu.

Conclusions

Electrical characterization of metal/SiLK/Si capacitors has been performed to address intrinsic material properties. The influence of the electrodes Al and Cu on the low-k SiLK, especially on the leakage behavior, has been compared by the BTS method with electrical measurements at varied temperatures. Two distinct conduction mechanisms of leakage current have been observed in the aromatic low-k polymer. The contact of metallic Al with the SiLK polymer will reveal the Schottky emission conduction on leakage behavior in the high electric field regions (>1 MV/cm). In contrast, as for Cu in contact with the low-k SiLK, copper plays a role in electrical trap center to assist carrier transport, leading to the PF-type leakage. Moreover, the tendency towards PF-type conduction is increasingly obvious with increasing temperatures because of the ease of copper diffusion into the SiLK film at high temperatures.

As known, Cu interconnects are typically clad with some sort of barrier layers in damascene technology; however, in case some variations in deposition process conditions occur and induce poor barrier properties, Cu ions are likely to penetrate the inadequate barriers into the low-k SiLK. Thus with proposed electrical analysis on leakage behavior, we can readily examine dielectric failure prior to material analysis steps. Therefore, the analysis technique will largely benefit monitoring process reliability of the Cu/low-k interconnects.

Acknowledgments

The authors are grateful to Dow Chemical Ltd. and Jay Hsu for SiLK preparation. This work was performed at the National Nano Device Laboratory and was supported by the National Science Council of the Republic of China under contract no. NSC 91-2721-2317-200.

The National Nano Device Laboratory assisted in meeting the publication costs of this article.

References

1. *International Technology Roadmap for Semiconductors*, Semiconductor Industry Association, San Jose, CA (1999).
2. P. A. Kohl, Q. Zhao, K. Patel, D. Schmidt, S. A. Bidstrup-Allen, R. Shick, and S. Jayaraman, in *Dielectric Material Integration for Microelectronics*, W. D. Brown, S. S. Ang, M. Loboda, B. Sammakia, R. Singh, and H. S. Rathore, Editors, PV 98-3, p. 169, The Electrochemical Society Proceedings Series, Pennington, NJ (1998).
3. P. T. Liu, T. C. Chang, Y. L. Yang, Y. F. Cheng and S. M. Sze, *IEEE Trans. Electron Devices*, **47**, 1733 (2000).
4. P. T. Liu, T. C. Chang, M. C. Huang, Y. L. Yang, Y. S. Mor, M. S. Tsai, H. Chung, J. Hou, and S. M. Sze, *J. Electrochem. Soc.*, **147**, 4313 (2000).
5. P. T. Liu, T. C. Chang, H. Su, Y. S. Mor, Y. L. Yang, H. Chung, J. Hou, and S. M. Sze, *J. Electrochem. Soc.*, **148**, F30 (2001).
6. P. T. Liu, T. C. Chang, Y. S. Mor, C. W. Chen, T. M. Tsai, C. J. Chu, F. M. Pan, and S. M. Sze, *Electrochem. Solid-State Lett.*, **5**, G11 (2002).
7. B. S. J. Martin, J. P. Godschalx, M. E. Mills, E. O. Shaffer II, and P. H. Townsend, *Adv. Mater.*, **12**, 1769 (2000).
8. R. D. Goldblatt, B. Agarwala, M. B. Anand, E. P. Barth, G. A. Biery, Z. G. Chen, S. Cohen, J. B. Connolly, A. Cowley, T. Dalton, S. K. Das, C. R. Davis, A. Deutsch, C. DeWan, D. C. Edelstein, P. A. Emmi, C. G. Faltermerier, J. A. Fitzsimmons, J. Hedrick, J. E. Heidenreich, C. K. Hu, J. P. Hummel, P. Jones, E. Kaltalioglu, B. E. Kastenmeier, M. Krishnan, W. F. Landers, E. Liniger, J. Liu, N. E. Lustig, S. Malhotra, D. K. Manger, V. McGahay, R. Mih, H. A. Nye, S. Purushothaman, H. A. Rathore, S. C. Seo, T. M. Shaw, A. H. Simon, T. A. Spooner, M. Stetter, R. A. Wachnik, and J. G. Ryan, in *Proceedings of the International Interconnect Technology Conference*, IEEE, p. 261, June 5-7, 2000.
9. J. J. Waeterloos, H. Struyf, J. V. Aelst, D. W. Castillo, S. Lucero, R. Caluwaerts, C. Alaerts, G. Mannaert, W. Boullart, E. Sleeckx, M. Schaekers, Z. Tokel, I. Vervoort, J. Steenbergen, B. Sijmus, I. Vos, M. Meuris, F. Iacopi, R. A. Donaton, M. V. Hove, S. Vanhaelemeersch, and K. Maex, in *Proceedings of the International Interconnect Technology Conference*, IEEE, p. 253, June 4-6, 2001.
10. R. Tsu, J. W. McPherson, and W. R. McKee, in *Proceedings of the International Reliability Physics Symposium*, IEEE, p. 348 (2000).
11. A. L. S. Loke, J. T. Wetzel, P. H. Townsend, T. Tanabe, R. N. Vrtis, M. P. Zussman, D. Kumar, C. Ryu, and S. S. Wong, *IEEE Trans. Electron Devices*, **46**, 2178 (1999).
12. S. M. Sze, *Physics of Semiconductor Devices*, p. 402, Wiley, New York (1981).